Available online at www.sciencedirect.com
SCIENCE DIRECT®
Journal of Catalysis 239 (2006) 354–361
JOURNAL OF CATALYSIS
www.elsevier.com/locate/jcat

Catalytically active states of Ru(0001) catalyst in CO oxidation reaction

R. Blume [a], M. Hävecker [a], S. Zafeiratos [a], D. Teschner [a], E. Kleimenov [a], A. Knop-Gericke [a], R. Schlögl [a], A. Barinov [b], P. Dudin [b], M. Kiskinova [b,*]

[a] *Fritz-Haber-Institut der Max-Planck-Gesellschaft, Faradayweg 4-6, 14195 Berlin, Germany*
[b] *Sincrotrone Trieste, AREA Science Park-Basovizza, Trieste 34012, Italy*

Received 24 January 2006; revised 11 February 2006; accepted 15 February 2006

Available online 20 March 2006

Abstract

Identifying the composition of the catalytically active state of metal catalysts under dynamic operating conditions is of particular importance for oxidation catalysis. Here we report new insights into the chemical identity of different catalytically active states formed on a Ru(0001) catalyst during CO oxidation at various reaction temperatures. The changes in the surface composition of the Ru catalyst and the CO_2 yield under varying reaction conditions in the 10^{-4}–10^{-1} mbar pressure range were followed in situ by synchrotron-based high-pressure X-ray photoelectron spectroscopy and mass spectroscopy. The results reveal that the catalytic activity of a few layers thick surface oxide without well-defined stoichiometry and structure is comparable with that of the stoichiometric $RuO_2(110)$ phase. This surface oxide forms under reaction conditions when RuO_2 formation is kinetically hindered and can coexist with RuO_2 in wide temperature and pressure ranges.

Keywords: CO oxidation; Ru; High pressure XPS; Catalytically active states

1. Introduction

Following the pioneering works demonstrating very high activity of the so-called O-rich Ru(0001) surface in CO oxidation [1,2], the rutile $RuO_2(110)$, formed on the Ru(0001) surface under realistic oxidation conditions, is considered the catalytically active state [3,4]. The rutile $RuO_2(110)$ surface consists of alternating rows of six-fold and unsaturated five-fold oxygen coordinated Ru atoms, with the latter, called cus-Ru, playing a prominent role as active sites in CO oxidation. The inspired UHV surface science and theoretical studies of CO oxidation reaction on a model $RuO_2(110)$ single-crystal surface reached the consensus that the elementary reaction steps involve CO and O adsorption on cus-Ru, followed by a reaction between cus-CO and cus- or bridge O atoms [5–9]. But the $RuO_2(110)$ surface is an idealised case of an active Ru catalyst, which has been prompted by the parallel studies focused on the oxidation mechanism of the Ru(0001) surface and the stability of the Ru oxidation states at various partial pressures and temperatures [10–16]. After completion of the O-(1×1) adsorption phase [17], the suggested oxidation pathway of the Ru(0001) surface involves as an important intermediate step the incorporation of O atoms between the first and second Ru layers and the formation of an O_{ad}–Ru–O_{sub} trilayer hosting 2 ML of oxygen [18,19], with 1 ML equalling the number of Ru atoms on the (0001) surface. The conversion into a $RuO_2(110)$ structure is supposed to occur above the critical thickness of two O–Ru–O trilayers (with an oxygen content of 4 ML). Spectroscopic evidence for subsurface oxygen species has been provided by photoelectron diffraction and combined photoemission and thermal desorption spectroscopy [20,21]. According to another model, based on investigations of Ru oxidation carried out at temperatures above 600 K, the RuO_2 nucleus is formed as long as the oxygen exceeds 1 ML, the coverage of the most dense (1×1) adsorption phase, and the $RuO_2(110)$ film grows progressively in an autocatalytic manner [10,22].

Recent XPS microscopy and TDS studies demonstrated that, starting from an atomically clean Ru(0001) surface, formation of a stoichiometric RuO_2 phase is kinetically hindered at temperatures below 500 K and occurs readily at higher tem-

* Corresponding author. Fax: +39 040 3758565.
E-mail addresses: kiskinov@fhi-berlin.mpg.de, kiskinova@elettra.trieste.it (M. Kiskinova).

0021-9517/$ – see front matter
doi:10.1016/j.jcat.2006.02.019

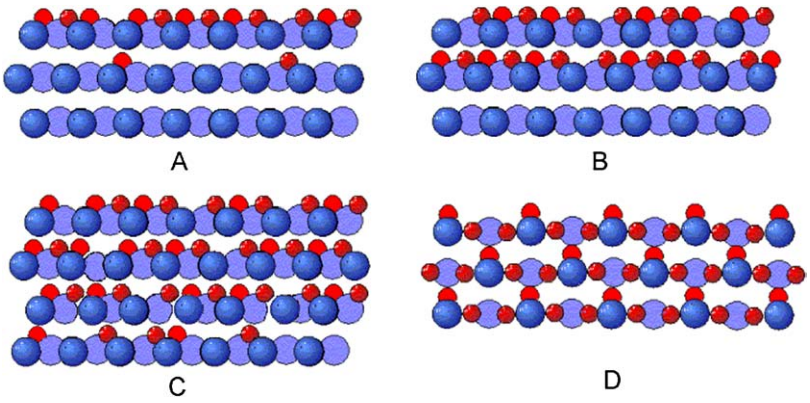

Fig. 1. Ball models of the oxidation states of Ru(0001), where O atoms are the small balls. (A) (1 × 1) saturated oxygen adsorption phase with ∼1 ML oxygen, the onset of subsurface O incorporation at $T \geqslant 400$ K; (B) "surface oxide" with ∼1 ML incorporated oxygen, the dominant phase formed at $T < 500$ K; (C) "surface oxide" with $\geqslant 2$ ML incorporated oxygen; (D) rutile $RuO_2(110)$ phase.

peratures [2,13,14,21]. The main reason for such temperature dependence of the Ru oxidation state is that the incorporation up to 3 ML of oxygen below 500 K is limited to the top two or three Ru layers. These O-rich thin films with poorly defined Ru_xO_y structure are called "surface oxides" and are identified as the precursor where the RuO_2 nucleates and grows at temperatures above 550 K.

Fig. 1 shows schematically the "oxidation" states of the Ru(0001) that have been proven experimentally [2,4,13,14,21]. In this paper we call these states the *adsorption phase*, referring to the state in which oxygen in present only on the surface with maximum coverage 1 ML (A); *surface oxide*, with ∼1–3 ML oxygen incorporated within the top few Ru layers (B and C); and *rutile* RuO_2 *phase* (D). An important finding of XPS microscopy is that the surface oxide and RuO_2 phases coexist in a wide temperature–pressure range, even when formed in a pure O_2 ambient [13,21]. Undoubtedly under reaction conditions, the CO will drive the oxidation state away from the equilibrium achieved in O_2 ambient, implying that the temperature–pressure space of coexistence of the two phases may be expanded.

The temperature dependence of the actual "oxidation" state and the morphology of the Ru surface reopen the disputable issue about the active state of Ru catalysts during CO oxidation. Here we use a specially built reaction chamber for simultaneous monitoring of the chemical state of the catalyst surface and the reaction product released in the gas phase at pressures up to a few mbar. We verified the catalytic activity of the different oxidation states of Ru(0001) catalyst, including the final stoichiometric RuO_2, starting from a metallic Ru surface and following in situ the temperature evolution of the catalyst surface composition in $CO + O_2$ environment close to the realistic oxidation, reduction, and steady-state reaction conditions.

2. Experimental

The experiments were performed in a high-pressure XPS station designed and constructed in FHI-MPG [23], attached to the beamline U49/2-PGM2 at the BESSY synchrotron radiation facility in Berlin. The overall energy resolution of the beamline was 0.1 eV at 500 eV. The photoelectron spectra were measured in situ using a setup combining differential pumping and electrostatic focusing of the emitted photoelectrons [24]. Briefly, the sample was mounted inside the reaction cell, 2 mm away from an aperture (1 mm diameter), which provided the entrance for the emitted photoelectrons and reaction products to the differentially pumped stages of the electrostatic lens system of the hemispherical analyser (Phoibos 150, SPECS GmbH). The gas-phase products, used to measure catalytic activity, were monitored on-line with a Hiden mass spectrometer located in the first differentially pumped lens stage. The sample was heated by a laser from the back side. The CO and O_2 gas flows into the reaction cell were regulated using leak valves.

The Ru(0001) sample was cleaned before each reaction cycle using well-established procedures [14,25]. The base pressure in the chamber was $\sim 2 \times 10^{-8}$ mbar, which reduced the lifetime of the atomically clean surface at room temperature. The temperature ramp was 2 K/min, and acquisition of a set of Ru 3d and O 1s spectra took a maximum of 4 min. Thus, the maximum difference between the temperatures at which the Ru 3d and O 1s spectra were taken was less than 8 K. All spectra were normalized to the incident photon flux, monitored by a photodiode with known quantum efficiency. The Ru 3d and O 1s spectra were measured with photon energies of 450 and 650 eV, respectively. Using the universal curve for the electron mean free path [26] the effective escape depths for the O 1s and Ru 3d photoelectrons was ∼5 Å, limiting the probing depth to the top few layers (∼10 Å). We also used higher photon energies to increase the probing depth when necessary.

3. Results and discussion

The experiments were carried out at different partial pressure ratios of CO and O_2 in the range of 10^{-4}–0.1 mbar. By varying the CO/O_2 pressure ratio, we could reproduce oxidation, reduction, and steady-state conditions of the working Ru catalyst. Simultaneous monitoring of the dynamic response of the O 1s and Ru $3d_{5/2}$ core-level spectra and the CO_2 production allowed us to correlate the catalytic activity to the actual oxidation state of the Ru catalyst.

Table 1
Energy positions of Ru $3d_{5/2}$ and O 1s components measured for the different oxidation states. The shift of the Ru $3d_{5/2}$ components with respect to the zero-energy reference (the position of the Ru $3d_{5/2}$ bulk component at 280.1 eV) is given in the brackets

State	Binding energy (eV)	Component	Ref.
Clean Ru	280.1 (0)	Ru_{bulk}	[25]
	279.75 (−0.35)	Ru(I)	[25]
	280.25 (0.15)	Ru(II)	[25]
Adsorbed phase	280.08	Ru(I)–$1O_{ad}$	[25]
	280.48 (0.4)	Ru(I)–$2O_{ad}$	[4,25]
	281.03 (0.93)	Ru(I)–$3O_{ad}$	[4,25]
RuO_2 phase	280.74 (0.64)	RuO_2-bulk	[4,13]
	280.45 (0.35)	Ru-cus	[27]
	283 (2.92)	Satellite	
"Surface oxide"	280.5 ± 0.05 (∼0.4)	Ru_xO_y	[21]
	280.6 ± 0.05 (∼0.8)	Ru(I)–$2O_{ad}O_{sub}$	[21]
	281.4 ± 0.05 (∼1.3)	Ru(I)–$3O_{ad}O_{sub}$	[21]
	280.9 ± 0.05 (∼0.5)	Ru(II)–O_{sub}	[21]
O 1s	530.0	O_{ad}& O_{sub}	[13]
	529.5	O in RuO_2-bulk	[4,13]
	528.7	"Bridge" O	[2]
O 1s–CO	530.8–531.8		[28]

The necessary basis for identifying the adsorption, surface oxide, and RuO_2 states and verifying their actual role in the CO oxidation reaction was provided by the already available Ru $3d_{5/2}$ and O 1s core level and TD spectroscopy data. The established binding energies of the Ru $3d_{5/2}$ and O 1s components corresponding to the adsorption state, surface oxide state, and rutile RuO_2 phase are summarized in Table 1.

The Ru(I) and Ru(II) components account for emission from the Ru atoms in the first and second layers, respectively. They undergo distinct chemical shifts when binding to O, determined by the coordination number of O atoms and their bonding configuration [4,25]. The incorporation of O subsurface, O_{sub}, leads to a distinct shift of Ru(II), resulting in the component Ru(II)–O_{sub} at ∼0.5 eV, well separated from the Ru_{bulk} position [21]. The Ru(I) energy shift induced by the subsurface oxygen accounts for the Ru(I)–$2O_{ad}O_{sub}$ and Ru(I)–$3O_{ad}O_{sub}$ components at ∼0.8 and 1.3 eV, assigned to the Ru(I) atom coordinated with two and three O adatoms, respectively, and subsurface oxygen below. When the total amount of adsorbed and incorporated oxygen exceeds ∼3 ML, a new broad component at ∼0.4 eV, Ru_xO_y, grows. This corresponds to the most advanced oxidation state below 500 K, with a poorly defined structure and thickness of about two rutile layers (5–6 Å) [21]. Although the energy position of the Ru_xO_y component is practically identical to that of the Ru(I)–$2O_{ad}$ component, the Ru 3d spectra are very different, because of the strong attenuation of Ru_{bulk} component due to screening by the surface oxide film. The RuO_2(110) phase has two components, corresponding to the cus-Ru and six-fold coordinated Ru atoms and a broad satellite at ≈283 eV [4,13,27]. The O 1s spectra from the adsorption and surface oxide states appear at 530.0 eV, with the latter being only a bit broader, indicative of multiple bonding configurations [13]. The O 1s spectrum of the RuO_2(110) phase has two components, reflecting the emission from the bridge O atoms at the RuO_2 surface (528.7 eV) and bulk RuO_2 oxygen (529.5 eV) [4,13]. The bridge oxygen component is clearly visible only when the RuO_2(110) surface is very well ordered and without oxygen vacancies. Because the bridge oxygen participates in the oxidation reactions [9,10], the corresponding O 1s component should be strongly reduced in ambient CO.

We evaluated the presence of adsorbed CO from the O 1s spectra, because the C 1s peak overlaps with the Ru $3d_{3/2}$ core level. The O 1s peaks of CO have binding energies between 530.8 and 531.8 eV and can be easily resolved from those of adsorbed oxygen and oxide [28].

3.1. Reduction of the surface oxide and RuO_2

The surface oxide stage (Fig. 2) and stoichiometric RuO_2 phase (Fig. 3) were formed by exposing Ru(0001) to 5×10^{-2} mbar O_2 at 450 and 620 K, respectively. The surface oxide contained ∼1.5–2.0 ML oxygen located on the surface and between the top and second Ru layers. The experiments were carried out in the 10^{-4} mbar range at CO/O_2 partial pressure ratio of 4, that is, in excess of CO. The reduction rate was compatible with simultaneous monitoring of the XPS and mass spectra, while slowly increasing the sample temperature, starting at 370 K. The results provide the necessary basis for understanding and interpretating the in situ CO oxidation data.

Fig. 2a shows representative Ru $3d_{5/2}$ spectra obtained during reduction of surface oxide. The bottom Ru $3d_{5/2}$ spectrum is of a "clean" Ru surface, before exposure to 1×10^{-2} mbar O_2 at 450 K. Although some CO from residual gas adsorbs on the surface at 2×10^{-8} mbar base pressure, its coverage is relatively low at 450 K, and the surface component Ru(I) is still present. For deconvolution, we used a broader component to account for the bulk and Ru(II) contributions. The Ru $3d_{5/2}$ spectrum of the surface oxide before the reaction contains components at ∼0.5, 0.8, and at 1.3 eV, which appear only in the presence of about 1 ML of incorporated oxygen [21]. Our previous XPS microscopy results did not show significant lateral inhomogeneity for such low-temperature oxidation states [21]. The broad O 1s spectrum in the bottom Fig. 2b peaks at 530.0 eV, corresponding to surface oxide.

The onset of reduction was at ∼390 K with a maximum CO_2 yield at ∼420 K, followed by a rapid decay to zero at ∼450–470 K. This leads to a decrease of the O 1s signal (Fig. 2c) and significant changes in the Ru $3d_{5/2}$ spectrum; the Ru_{bulk} grows, accompanied by rapid attenuation of the Ru(I)–$2O_{ad}O_{sub}$ at 0.8 eV, whereas the Ru(II)–O_{sub} at 0.5 eV broadens and gradually shifts to 0.4 eV, the position of the Ru(I)–$2O_{ad}$ component. These results indicate that once the oxygen from the surface is consumed, the limited amount of oxygen incorporated between the first and second layers is thermodynamically driven to segregate to the surface [18]. Thus the system converts into an oxygen adsorption phase. A peculiar feature in the evolution of the Ru $3d_{5/2}$ spectra is that the Ru(I)–$3O_{ad}$ component at 0.9 eV does not gain sensible intensity, indicating direct reduction of the surface oxide into an adsorption state with moderate oxygen coverage of ∼0.7 ML.

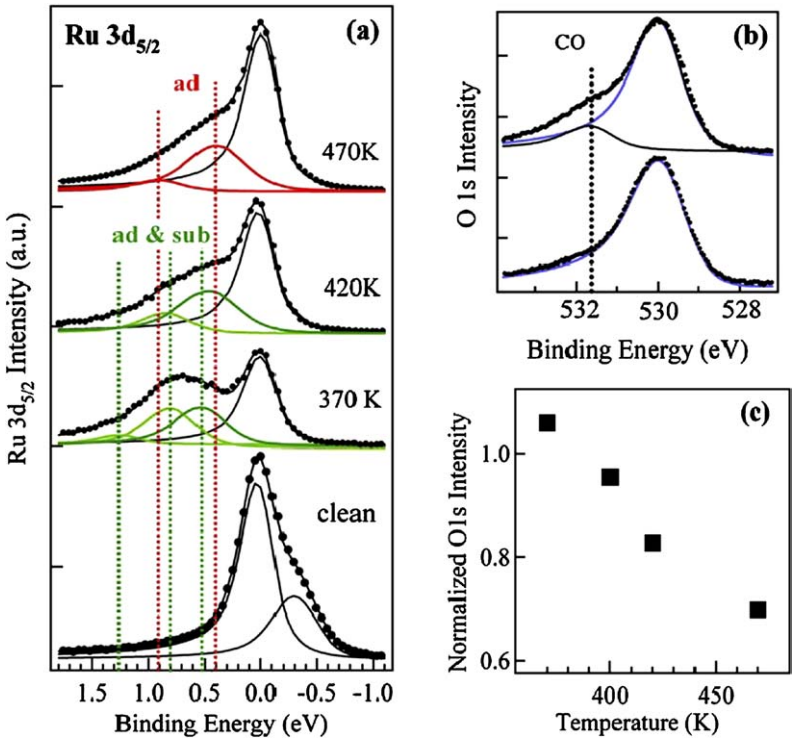

Fig. 2. (a) From bottom to top: Ru $3d_{5/2}$ spectra taken before exposure to O_2, after oxidation at 450 K and cooling the "surface oxide" to 370 K and following reduction with increasing the temperature. The "ad & sub" annotation indicates the three components, Ru(I)–$3O_{ad}O_{sub}$, Ru(I)–$2O_{ad}O_{sub}$, and Ru(II)–O_{sub}, which are fingerprints of the O-rich state with incorporated oxygen. (b) O 1s spectra taken after oxidation at 450 K (bottom) and after exposure of this surface to CO at 320 K (top). (c) O 1s intensity as a function of reduction temperature. The O 1s signal is normalised assuming that the intensity of the adsorption phase corresponds to 0.7 ML. $dT/dt = 2°/\text{min}$. Reduction conditions: $p_{CO} = 2 \times 10^{-4}$ mbar, $p_{O_2} = 0.5 \times 10^{-4}$ mbar.

Simple calculations, considering the electron escape depth for our experimental setup, predict that for surface oxide with an initial load of 2 ML, the reduction to 0.7 ML adsorption phase should cause a ∼50% decrease in O 1s intensity (1 ML subsurface oxygen contributes to ∼30% of the initial signal). The experimentally measured decrease in O 1s intensity of ∼35% indicates that the total initial load of oxygen within the top two Ru layers is somewhat less than 2 ML. In fact, the Ru(I)–$3O_{ad}O_{sub}$ component at ∼1.3 eV is already rather weak in the Ru $3d_{5/2}$ spectra from the surface oxide before the reduction, compatible with the presence of vacancies on the surface. This finding also is consistent with the evolution of the Ru $3d_{5/2}$ spectra during the reduction, which does not pass through a saturated adsorption layer of 1 ML. One possible explanation is that once the oxygen starts to incorporate below the surface, it naturally leaves vacancies on the surface [18,29] where CO can stick and react. Indeed, when the freshly formed surface oxide was cooled to 370 K and exposed to ambient CO, a shoulder at about 531.7 eV grows in the O 1s spectrum due to adsorption of CO molecules (Fig. 2b). By varying the CO/O pressure ratio, the initial surface oxide can be restored under oxidizing conditions at 450 K, whereas under reducing conditions, the adsorbed O can be further depleted only at temperatures above 600 K, which leaves a diluted adsorption state with mostly single coordinated Ru atoms.

The Ru $3d_{5/2}$ spectrum after oxidation in 10^{-2} mbar O_2 at 620 K (Fig. 3a) did not contain a Ru_{bulk} component, even when measured using photon energies of 1000 eV, which increased the probing depth. This indicates that the stoichiometric RuO_2 film formed is thicker than ∼15 Å. The bulk oxide component dominates the spectra, but the Ru-cus component is also present, suggesting a uniform and structured RuO_2(110) surface. The O 1s spectrum in Fig. 3b peaks at 529.5 eV, as expected for the RuO_2 phase, with broadening on the side of the bridge O surface component at 528.7 eV [4,13].

CO_2 formation starts at ∼420 K and is marked by the appearance and growth of the Ru_{bulk} component with increasing reaction temperature and decreasing O 1s intensity. As illustrated by the plot in Fig. 3c, the most rapid loss of O 1s intensity occurs at ∼450–470 K, where the maximum CO_2 yield was monitored. The evolution of the Ru $3d_{5/2}$ spectra in Fig. 3a illustrates how the ongoing reaction continuously consumes the oxide. Above ∼520 K, the Ru(I)–$2O_{ad}$ component begins to grow as well, accompanied by an accelerated increase in the Ru_{bulk} and attenuation of the oxide component. This indicates a patchy morphology of the surface, consisting of diminishing oxide islands and inactive adsorption phase. Above ∼580 K, the Ru $3d_{5/2}$ spectrum becomes almost identical to that of the inactive adsorption state with ∼0.7 ML of oxygen, achieved during reduction of the surface oxide (see Fig. 2a). The apparent direct conversion from RuO_2 to an inactive adsorption phase is supported by the evolution of the RuO_2 satellite (not shown), distinguishable in the Ru 3d spectra up to ∼550 K. This is consistent with the results in Fig. 2 showing that the surface oxide is unstable at temperature above 500 K under reduction condi-

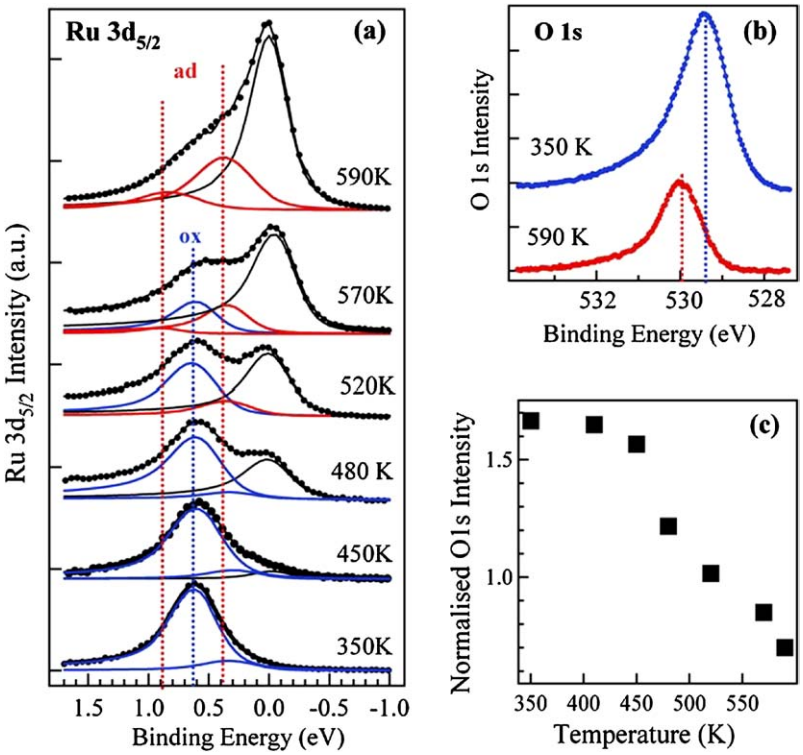

Fig. 3. (a) From bottom to top: Ru $3d_{5/2}$ spectra taken after oxidation at 620 K and cooling to 350 K, and following reduction with increasing the temperature. (b) O 1s spectra taken before introducing CO (top) and after reduction to adsorption phase (bottom). (c) O 1s intensity changes with increasing the reduction temperature. The O 1s signal is normalised against the intensity of the adsorption phase, corresponding to 0.7 ML. $dT/dt = 2$ K/min. Reduction conditions: $p_{CO} = 2 \times 10^{-4}$ mbar, $p_{O_2} = 0.5 \times 10^{-4}$ mbar.

tions, as well as Fig. 3b showing the shift in the O 1s spectrum to 530.0 eV.

In brief, the stabilities of the surface oxide and the stoichiometric RuO_2 under reduction condition appear comparable; both can be easily reduced in excess of CO in the gas phase mixture at temperature above 400 K and the final reduced state at temperature below 600 K is the same inactive adsorption phase with ∼0.7 ML of oxygen. It should be noted that in surface science experiments, carried out far from realistic temperature and pressure conditions, no reduction of the $RuO_2(110)$ was observed even in extreme excess of CO (i.e., CO/O_2 pressure ratios of 10) [7].

3.2. Catalytically active transient states of Ru surface during CO oxidation at different temperatures

The experiments were carried out at 0.1 mbar and a CO/O_2 partial pressure ratio of 1. We started with a clean Ru(0001) surface and slowly increased the temperature after introducing the reactants in the gas phase. The excess of oxygen with respect to the reaction stoichiometry provided slightly oxidizing conditions to ensure the formation of stoichiometric RuO_2 above 500 K, which did not readily occur when using a stoichiometric CO/O_2 ratio of 2. Another reason for choosing this CO/O_2 ratio is that the highest turnover rates over working Ru catalysts under realistic conditions were measured at about equal partial pressures of the reactants [30].

The mass spectrometry and XPS data allowed us to correlate the CO_2 yield and oxidation state of the catalyst at different reaction temperatures, ranging from 370 to 600 K. Fig. 4a shows the evolution of the CO_2 yield with increasing reaction temperature. The plot has three distinct regions: a very weak increase up to ∼420 K, a sharp onset of the oxidation reaction at ∼420 K with a continuously increasing CO_2 yield up to ∼550 K, followed by a flat maximum and slow decline above ∼580 K.

The evolution of the Ru oxidation state with increasing reaction temperature is illustrated by the selected O 1s and Ru $3d_{5/2}$ spectra in Figs. 5a and b. The surface composition of Ru catalyst in the $CO + O_2$ ambient at temperatures before the sharp onset of the CO_2 production is best represented by the O 1s spectra Fig. 5a, taken at temperatures below 420 K. They clearly show the presence of CO on the surface (component at ∼531.7 eV) up to ∼400 K. CO removal at 400–420 K is accompanied by some loss in O 1s intensity at 530.0 eV, assigned to surface and subsurface oxygen, and by a weak increase in the CO_2 yield. This suggests that the adsorbed CO reacts with surface O and leaves the surface as CO_2. This scenario is in accordance with the Ru $3d_{5/2}$ spectrum in Fig. 5b taken at 395 K, where the absence of Ru(I)–$2O_{ad}O_{sub}$ component indicates that the O surface coverage is substantially reduced after the removal of CO. We did not consider here the Ru $3d_{5/2}$ spectrum before CO removal, because of the unknown effect of the CO on the surface core level position. The O 1s peak at 530.0 eV gains intensity above 400 K, indicating further accumulation of oxygen; this also leads to the increase of Ru(II)–O_{sub} and

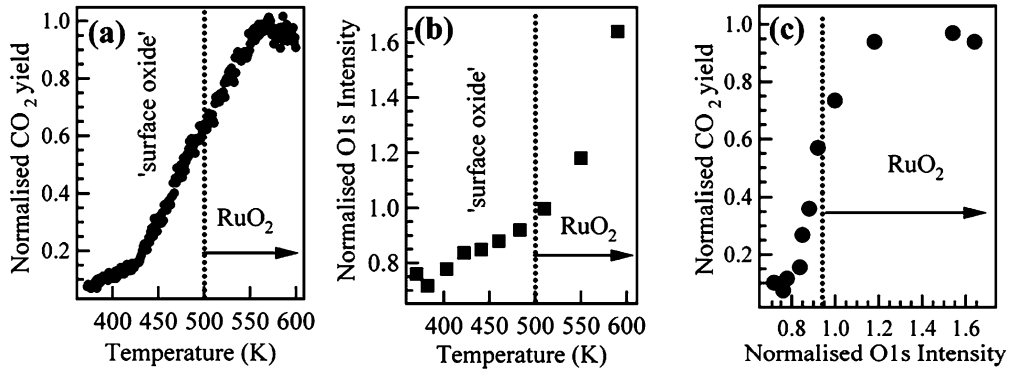

Fig. 4. (a) CO_2 yield as a function of reaction temperature. (b) O 1s intensity after subtraction of the CO contribution as a function of reaction temperature. The O 1s signal is normalised as in the reduction experiments (see Figs. 3b and 2b). The O 1s intensity up to ∼500 K reflects only the surface and subsurface content, whereas above 500 K the increase is dominated by the formation of an RuO_2 phase. (c) Plot of the CO_2 yield versus O content at the surface and near surface region. The dashed line in (a)–(c) indicates the onset of the RuO_2 growth.

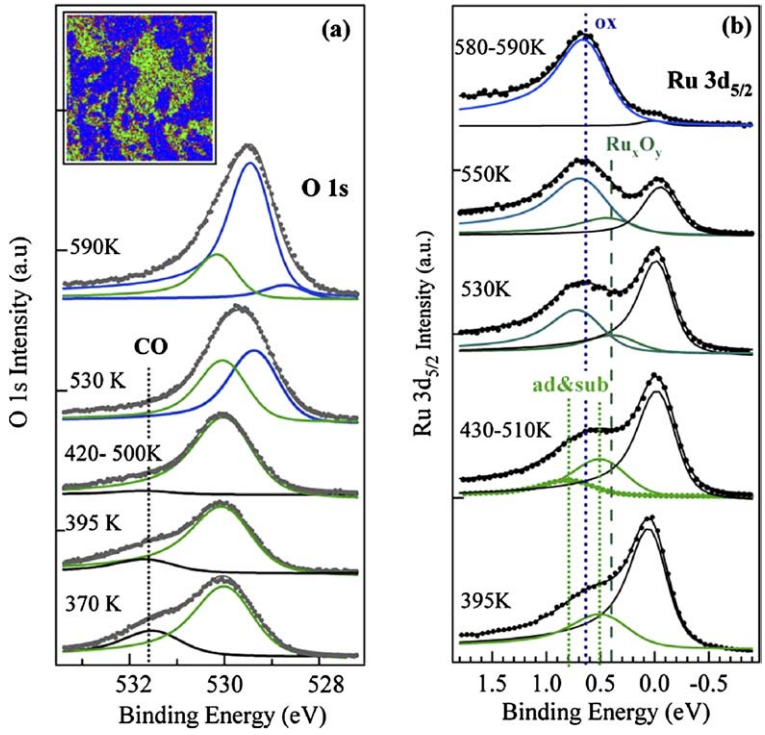

Fig. 5. (a) Ru $3d_{5/2}$ (a) and O 1s (b) spectra illustrating the catalyst composition developed during CO oxidation with increasing of the reaction temperature from 370 to 600 K. $dT/dt = 2$ K/min. Reaction conditions: $p_{CO} = 0.5 \times 10^{-1}$ mbar, $p_{O_2} = 0.5 \times 10^{-1}$ mbar. The insert in (a) is a Ru 3d map illustrating the surface morphology developed after exposure to 10^6 L O_2 at 670 K with RuO_2 (dark) and Ru_xO_y (bright) islands.

Ru(I)–$2O_{ad}O_{sub}$ components in the Ru $3d_{5/2}$ spectra. The Ru $3d_{5/2}$ and O 1s spectra undergo negligible line shape changes at 420–500 K, despite the continuous increase in CO_2 yield. The deconvoluted Ru $3d_{5/2}$ spectra have a dominant Ru(II)–O_{sub} component at 0.5 eV and a rather weak Ru(I)–$2O_{ad}O_{sub}$ component at 0.8 eV. This means that under the actual operational conditions, the catalyst contains a significant amount of subsurface oxygen, whereas the O species on the surface are effectively consumed by the ongoing reaction. The rapid dynamics at the surface is confirmed by the practical absence of CO-related feature in the O 1s spectra, indicating a short lifetime of the CO species on the surface before being reacted off.

Because the CO_2 formation reaction cannot disturb the surface composition to any significant degree, the observed temperature dependence of the reaction rate is most likely related to further accumulation of oxygen, facilitated at higher temperatures. This accounts for the slow gradual increase in O 1s intensity below 500 K, as illustrated in Fig. 4b. In this context, we note that the lattice stress induced by incorporation of O produces local changes in both the geometric and electronic structures of the top Ru layer [18,31], thereby affecting the Ru–O and Ru–CO adsorption bond and/or modifying the adsorbate bonding configurations. As a result, the barrier to achieve the transition CO–O state may be reduced, increasing surface activity and CO_2 yield.

A natural consequence of the progressive incorporation of oxygen with further increases in reaction temperature is the nucleation and growth of stoichiometric RuO_2. Indeed, the Ru $3d_{5/2}$ spectra in Fig. 5b undergo significant changes above 500 K, due to formation of RuO_2 until a steady-state composition is reached and maintained in the 550–600 K range. A weak Ru_{bulk} component can still be distinguished in the Ru $3d_{5/2}$ spectrum of this steady-state, compared with much thicker RuO_2 films grown in pure O_2 ambient (see Fig. 3a). This indicates that RuO_2 growth is slower during CO oxidation, reflecting the kinetic limitations imposed by the presence of CO. Based on our XPS microscopy findings [13], the hindered oxide growth should result in a patchy structure consisting of RuO_2 islands and Ru_xO_y areas, with the latter accounting for the presence of the Ru_{bulk} component. A typical morphology of such a surface is illustrated by the Ru $3d_{5/2}$ image in the O 1s panel (Fig. 5a). The RuO_2 islands appear dark, because the RuO_2 phase contains less Ru atoms per unit volume than the adsorption and O-rich intermediate states (bright) and also, being thicker, it more effectively screens the emission from the metallic Ru below. Similar coexistence of the two phases was observed in very wide temperature range (600–775 K) and exposure range [13,21]. Because the Ru_xO_y component appears close to the cus-Ru component of the $RuO_2(110)$ surface (see Table 1), and it is speculative to fit the Ru $3d_{5/2}$ spectra using three components with unknown weight, we allowed a broadening of the dominant oxide component at ∼0.6 eV to account for all contributions. The coexistence of the both oxidation states is confirmed by the corresponding O 1s spectrum, which contains the surface oxide and RuO_2 components. Judging from the relative weight of the surface oxide O 1s component, about 80% of the surface should be covered with RuO_2 islands at 590 K. Note that the RuO_2 bridge O component at 528.7 eV is very weak, probably due to its continuous consumption during the reaction, in accordance with the mechanism suggested in previous work [7,9]. The reaction rate can be reverted back and forth by decreasing and increasing the temperature in the range of 550–600 K, which does not visibly affect the catalyst surface composition.

The most striking result is that the growth of the RuO_2 phase above 500 K does not affect the monotonous increase of the CO_2 yield (Fig. 4a). This suggests that the nucleation and growth of a stoichiometric oxide phase barely affects the reaction barrier. The plot of the CO_2 yield versus O content in Fig. 4c provides the best illustration that the high catalytic activity of the Ru catalyst is not strongly correlated with the formation of RuO_2 with a well-defined surface structure. It clearly shows that the surface oxide formed via progressive incorporation of oxygen already exhibits high catalytic activity and that there is no significant increase with the formation of stoichiometric RuO_2. Here it should be noted that because RuO_2 formation occurs above 500 K, when comparing the catalytic activity of the surface oxide and RuO_2, the positive temperature effect on the reaction rate should be taken into account as well.

The fact of the coexistence of surface oxide and RuO_2 states does not produce unambiguous results correlating the CO_2 yield with a single phase by running the reaction at a constant temperature above 500 K, where RuO_2 nucleation and growth occur. However, the catalytic activity of the surface oxide was confirmed by recent experiments performed using a stoichiometric CO/O_2 partial pressure ratio of 2 instead of 1, maintaining the same total pressure of 0.1 mbar. We increased the temperature from 400 to 600 K in 20–25 K steps, waiting at each new temperature until the CO_2 signal reached a constant value. In this case the higher CO/O_2 gas pressure ratio hindered formation of the RuO_2 state, as indicated by the evolution of Ru 3d and O 1s spectra, which terminated at the formation of surface oxide. The CO_2 yield grew steadily, showing stable activity at constant temperature, until levelling off at around 500 K and declining slowly above 550 K. This result is in qualitative agreement with the results with powdered Ru catalyst, which demonstrate that an ultra-thin oxide layer covering the metallic Ru core is the active state in CO oxidation at temperatures below 500 K [32].

4. Conclusion

The in situ capability of high-pressure photoelectron spectroscopy has provided real-time information about the evolution of the chemical state of Ru(0001) catalyst during CO oxidation with increasing reaction temperature. The results confirm that the metallic state of Ru is inactive. The most important finding is that the CO_2 production is not phase-selective; that is, there is no distinct difference in catalytic activity between the stoichiometric $RuO_2(110)$ and a few layers thick, poorly ordered surface oxide.

According to density functional theory predictions, the higher catalytic activity of an oxide surface compared with the corresponding metal surface not only results from the weaker CO and O bonding on the oxide; an important and in some cases even decisive role is the reorganisation required to achieve the configuration of the transition state [16]. In the frame of this concept, the activation role of the subsurface oxygen should be ascribed to the induced deformation of the lattice, which affects the O and CO adsorption configurations. The growth of stoichiometric RuO_2 does not substantially change the reaction barrier. This result is not surprising, because, as noted above, the activity is determined by the O and CO bonding configurations on the catalyst surface. Apparently, the amorphous surface oxide formed below 500 K has attained a favourable structure with activity comparable to that exhibited by the well-defined RuO_2 phase formed at higher temperatures.

In CO excess, the limited amount of subsurface oxygen is energetically driven to segregate to the surface, and the amorphous surface oxide can easily lose the incorporated oxygen and convert into an inactive adsorption phase. However, the RuO_2 also is unstable in CO excess and, similar to the surface oxide, can be reduced into an inactive adsorption phase; however, reoxidising the reduced catalyst back to the initial stoichiometric RuO_2 is not necessary to regain catalytic activity.

The surface-phase diagram of the $RuO_2(110)$ surface, reported previously [6], considers that the catalytically active region under realistic dynamic reaction conditions can often lie

at the boundary between two phases. The present study provides experimental evidence that the highest CO oxidation rate is monitored in the temperature range of 500–600 K, at which two Ru oxidation states coexist.

The results of this work apply well to real Ru catalyst systems, which are nanoparticles forming amorphous oxide with poorly defined stoichiometry [33,34]. Such "oxidized" states of the Ru nanoparticles, often described as Ru_xO_y, are comparable with surface oxide with subsurface oxygen, not with the well-structured $RuO_2(110)$ surface. This study conforms that RuO_2 formed at temperatures above 500 K is also active but represents a limiting case of a well-ordered model structure. The long-range ordering of the $RuO_2(110)$ surface is not a prerequisite for catalytic function, but is instrumental in unravelling and providing insight into the mechanisms of CO oxidation at the atomic level. As noted above, a recent study of the CO oxidation on polycrystalline powdered Ru catalyst in the temperature range of 363–453 K showed that under dynamic catalytic conditions, the active state is an ultra-thin Ru oxide film, whereas fully oxidized RuO_2 particles, formed at higher temperature, exhibit lower activity [32]. This deactivation is tentatively attributed to roughening and formation of inactive RuO_2 facets.

In general, the long-range ordered oxide structures available in macroscopic systems cannot be the ones working under conditions of high chemical potential and enabled structural dynamics (real world). However, they are excellent model systems for fundamental experimental and theoretical studies of catalytic reactions, helping to identify the general reactivity trend on metallic and O-rich states of catalysts used in redox processes.

Acknowledgments

The authors are indebted to Dr. W. Ranke for providing a critical reading of the manuscript and engaging in illuminating discussions. M. Kiskinova thanks the AvH Foundation for an award to pursue research in FHI-Berlin in 2004–2005. P. Dudin acknowledges financial support under contract NMP3-CT-2003-505670 (NANO2). The BESSY staff is acknowledged for their continuous support in performing the present measurements.

References

[1] A. Böttcher, H. Niehus, S. Schwegmann, H. Over, G. Ertl, J. Phys. Chem. B 101 (1997) 11185.
[2] A. Böttcher, H. Niehus, J. Chem. Phys. 110 (1999) 3186, Phys. Rev. B 60 (1999) 14396.
[3] H. Over, Y.D. Kim, A.P. Seitsonen, E. Lundgren, M. Schmid, P. Varga, A. Morgante, G. Ertl, Science 287 (2000) 1474.
[4] H. Over, A.P. Seitsonen, E. Lundgren, M. Wiklund, J.N. Andersen, Chem. Phys. Lett. 342 (2001) 467.
[5] Z.-P. Liu, P. Hu, A. Alavi, J. Chem. Phys. 114 (2001) 5956.
[6] K. Reuter, M. Scheffler, Phys. Rev. Lett. 90 (2003) 46103, Phys. Rev. B 60 (2003) 45407.
[7] J. Wang, V.Y. Fan, K. Jacobi, G. Ertl, J. Phys. Chem. B 106 (2002) 3422.
[8] S.H. Kim, J. Wintterlin, J. Chem. Phys. B 108 (2004) 14565.
[9] K. Reuter, D. Frenken, M. Scheffler, Phys. Rev. Lett. 93 (2004) 116105.
[10] H. Over, M. Muhler, Prog. Surf. Sci. 72 (2003) 3, and references therein.
[11] H. Over, M. Knapp, E. Lundgren, A.P. Seitsonen, M. Schmid, P. Varga, Chem. Phys. Chem. 5 (2004) 167, and references therein.
[12] Y.D. Kim, H. Over, G. Krabbes, G. Ertl, Top. Catal. 14 (2001) 95.
[13] A. Böttcher, U. Starke, H. Conrad, R. Blume, L. Gregoriatti, B. Kaulich, A. Barinov, M. Kiskinova, J. Chem. Phys. 117 (2002) 8104.
[14] R. Blume, H. Niehus, H. Conrad, A. Böttcher, J. Phys. Chem. 108 (2004) 14332.
[15] A. Böttcher, B. Krenzer, H. Conrad, H. Niehus, Surf. Sci. 504 (2002) 42.
[16] X.-Q. Gong, Z.-P. Liu, R. Raval, P. Hu, J. Amer. Chem. Soc. 126 (2004) 8.
[17] One monolayer equals the number of Ru atoms on the (0001) surface. We use in further as an unit to express the total O load
[18] M. Todorova, W.X. Li, M.V. Ganduglia-Pirovano, C. Stampfl, K. Reuter, M. Scheffler, Phys. Rev. Lett. 89 (2002) 96103.
[19] K. Reuter, C. Stampfl, M.V. Ganduglia-Pirovano, M. Scheffler, Chem. Phys. Lett. 352 (2002) 311.
[20] P. Quinn, D. Brown, D.P. Woodruff, T.C.Q. Noakes, P. Bailey, Surf. Sci. 491 (2001) 208.
[21] R. Blume, H. Niehus, H. Conrad, A. Böttcher, L. Aballe, L. Gregoriatti, A. Barinov, M. Kiskinova, J. Phys. Chem. B 109 (2005) 14052.
[22] H. Over, A.P. Seitsonen, Science 297 (2002) 2003.
[23] H. Bluhm, M. Hävecker, A. Knop-Gericke, E. Kleimenov, R. Schlögl, D. Teschner, V.I. Bukhtiyarov, D.F. Ogletree, M. Salmeron, J. Phys. Chem. B 108 (2004) 14340.
[24] D.F. Ogletree, H. Bluhm, C. Lebedev, C.S. Fadley, Z. Hussain, M. Salmeron, Rev. Sci. Instrum. 73 (2002) 3872.
[25] S. Lizzit, A. Baraldi, A. Groso, K. Reuter, M.V. Ganduglia-Pirovano, C. Stampfl, M. Scheffler, M. Stichler, C. Keller, W. Würth, D. Menzel, Phys. Rev. B 63 (2001) 205419.
[26] M.P. Seah, Surf. Interface Anal. 9 (1986) 85.
[27] H. Over, A.P. Seitsonen, E. Lundgren, M. Smedh, J.N. Anderesen, Surf. Sci. 504 (2002) L196.
[28] A. Schiffer, P. Jacob, D. Menzel, Surf. Sci. 389 (1997) 116.
[29] W.X. Li, C. Stampfl, M. Scheffler, Phys. Rev. B 67 (2003) 45408.
[30] C.H. F Peden, D.W. Goodman, J. Phys. Chem. 90 (1986) 1360.
[31] M. Mavrikakis, B. Hammer, J.K. Norskov, Phys. Rev. Lett. 81 (1998) 2819.
[32] V. Narkhede, J. Assmann, M. Muhler, Z. Phys. Chem. 219 (2005) 979.
[33] W. Vogel, N. Alonso-Vante, J. Catal. 232 (2005) 395.
[34] B.-Z. Zhan, M.A. White, T.-K. Sham, J.A. Pincock, R.J. Doucet, K.V. Ramana Rao, K.N. Robertson, T.S. Cameron, J. Amer. Chem. Soc. 125 (2003) 2195.